ISSN 2320 2599

Volume 1, No.1, November – December 2012
International Journal of Microwaves Applications
Available Online at http://warse.org/pdfs/ijma03112012.pdf

PIC Simulation of a Gyro-TWT Amplifier to Study its Beam-Wave Interaction Behavior

M.Thottappan[1], P.K.Jain[2]
Centre of Research in Microwave Tubes, Department of Electronics Engineering,
Indian Institute of Technology (Banaras Hindu University),
Varanasi– 221 005, INDIA.
Email:arul_saro1988@yahoo.co.in[1], pkjain_crmt@sify.com[2]

ABSTRACT

In this paper, PIC simulation of a Ka-band gyro-TWT amplifier is presented to study the electron beam and RF wave interaction behavior in the device. The lossy dielectrics have been periodically placed in the RF interaction structrure (usually smooth wall cylindrical waveguide) of the gyro-TWT so as to provide high attenuation to the potentially competing modes and also improve the device stability. The technique for generating the annular gyrating electron beam has been demonstrated using "CST particle studio" PIC simulation code and the energy transfer phenomenon from hot electron beam to the propagating electromagnetic wave has also been investigated. The performance of periodically dielectric loaded waveguide interaction structure has been monitored to ensure the device operation in the desired mode and frequency. The effect of beam velocity spread on the RF power output has also been illustrated. The PIC simulation code predicts that the peak output power in the dielectric loaded gyro-TWT is approximately 175 kW at 35 GHz corresponding to the power conversion efficiency of ~25% for a 70 keV, 10 A annular electron beam with a perpendicular to parallel velocity ratio of 1.0. The gain of the device is observed ~ 42 dB and the 3 dB instantaneous bandwidth is obtained ~ 6%. Further, it is observed that only the desired TE_{01} mode present in the RF output and other spurious competing modes, like, TE_{21}, TE_{31} and TE_{41} etc. have negligible growth.

Key words : Beam wave interaction, High power millimeter wave amplifier, Gyrotron traveling wave tube, PIC simulation.

1. INTRODUCTION

Traveling Wave Tube (TWT) amplifier power capability deceases with the increase of its operating frequency due to the decrease in its dimension. There are need for high power and broadband amplifier for many applications which includes the atmospheric propagation window near 35 and 94 GHz [1]. In contrast to conventional microwave tubes, gyrotron type devices which are based on the cyclotron resonance maser (CRM) instability can be used for the generation and amplification of high power millimeter waves. The Gyro-TWT is a fast wave microwave tubes works on the principle of CRM instability, involving the interaction of energetic gyrating relativistic electrons with a transverse waveguide mode. In the CRM devices, the coherent radiation is produced by the phase bunching of the mildly relativistic electrons gyrating in their Larmor orbits around the guiding center. When the interaction involves the gyrating motion of electrons in a static magnetic field 'B_0', the synchronism requires that

$$\omega - k_z v_z - s\Omega_c \approx 0 \qquad (1)$$

where, ω is the wave frequency, k_z is the propagation constant, v_z is the electron axial velocity, s is the cyclotron harmonic number and Ω_c is the relativistic electron cyclotron frequency. Here, one can use overmoded smooth wall cylindrical waveguide as RF interaction circuit, thereby much larger dimension structure could be used. By and large, the ECM-based devices have a unique position in the millimeter and sub millimeter wavelength regime of the electromagnetic spectrum, due to their unprecedented power development levels, and consequently which are found to be used in numerous applications like high resolution radars imaging radrs, high density communication systems, particle acceleration, materials characterization, plasma heating and solid state diagnostics, tracking of space substances, linear colliders, power beaming and electron cyclotron resonance heating of fusion plasmas, etc.

A gyro-TWT having traveling wave circuit is capable of providing much wider bandwidth. Unfortunately, gyro-TWTs have been overwhelmed by instabilities and hence the fundamental mode of operation of these devices is also limited to lower frequencies due to its large requirement of magnetic field strengths [2]. These oscillations are mainly categorized into reflective oscillations due to reflections at the input–output couplers and structural non uniformity, the

absolute instability near the cutoff frequency of the operating mode, and gyrotron backward-wave-oscillations (gyro-BWO). In one of the first gyro-TWTs [3], oscillation at the cutoff frequency due to an absolute instability [4] forced the device to be strongly detuned, which lowered the gain and bandwidth. The performance was improved by making the walls of the interaction circuit is more lossy [5]. The stability of the gyro-TWT can be achieved by increasing the wall load in the interaction region. In the last two decades, a number of experimental studies of the gyro-TWT have been reported. In 1996, Q.S.Wang *et.al.* at University of California, Davis experimented a single stage ku-band second harmonic gyro-TWT with an axial cut cylindrical waveguide interaction circuit which has developed an output power of 207 kW, the large and small signal gains of 16 dB and 38 dB respectively. The saturated bandwidth was obtained as 2.1 % [6]. In 1998, at the National Tsing Hua University (NTHU) K.R.Chu *et.al*. have studied experimentally an ultra-high gain gyro-TWT amplifier with distributed lossy interaction circuit, which produced the saturated peak power of 93 kW, 70 dB ultra high gain, 26.5% efficiency, and a 3 dB bandwidth of 3 GHz [7]. This unprecedented gain suppresses spurious oscillations. In the year of 1999, a second harmonic gyro-TWT with a helically corrugated interaction circuit was developed by Russian and United Kingdom researchers and which has produced a maximum output power of 1.1 MW, and an instantaneous 3 dB relative bandwidth of nearly 21% (8.4 to 10.4 GHz) [8]. In 2002, J.P.Calame *et.al*. have achieved the peak powers of 125–140 kW at about 49 dB saturated gain with a lossy ceramic interaction circuit in the same laboratory [9]. The stability of this device was excellent, demonstrating that ceramic loading is a highly effective means of suppressing spurious oscillations in gyro-TWTs.

One of the most effective methods to suppress the above mentioned oscillations is the use of distributed-loss technology. The distributed-loss circuit for beam wave interaction consists of a long lossy section (namely, the linearly loaded section) and a short conducting-wall section (namely, nonlinearly unloaded section). Another effective method to overcome absolute instability and Gyro-BWO is a sever circuit which is commonly used in the conventional TWT. The periodic dielectric loading approach has been identified as a suitable candidate to have superior stability characteristics in Gyro-TWT amplifiers as compared to that using a localized lossy severs [6],[7].

This paper describes the PIC simulation of a high performance 35-GHz TE_{01} mode gyro-TWT that applies the same technique of employing a periodic dielectric loaded interaction section to achieve stability as mentioned in [10]. The TE_{01} mode is employed because its low loss in the output section could potentially allow the amplifier to be operated at high average power and its radial maximum at halfway between the wall and center is ideal for the placement of the electron beam. The remainder of the paper is organized as follows. The Section 2 gives the details of the Particle In Cell (PIC) simulation code and the modeling of cathode and the interaction structure. Section 3 shows the simulation results obtained by both cold analysis and PIC simulation techniques. The Section 4 presents the performance evaluation of the Gyro-TWT at 35 GHz using parametric analysis. At last, the results are summarized and conclusions are drawn in Section 5.

2. DESCRIPTION OF PIC SIMULATION

Although, the studies of electromagnetic (EM) wave amplification in devices based on the cyclotron-maser instability were started in the late 1950s [11], the various numerical codes appeared which are widely used nowadays for the analysis and design of gyro-TWTs [7], [12], [13]. Recently, advances in the code development were reviewed by T.M Antonsen Jr. *et al*. [14]. The CST particle studio is a module for carrying out the simulation of interaction mechanism between electromagnetic fields and charged particles. It is based on the Finite Integration (FI) technique and uses hexahedral/tetrahedral meshing for discretizing the solution of interest region. The diagnosis of results and its post-processing module are its salient features. Another PIC code is MAGIC which is a user configurable code which is based on Finite-Difference Time-Domain (FDTD) method while CST particle studio is GUI based 3D simulation code. The limitation of MAGIC software is that the output power corresponding to only one mode could be observed and it is not possible to observe the power levels of the other competing modes which are present in the output port.

2.1 Modeling of the Interaction Circuit

The foremost part of a gyro-TWT is its interaction circuit. This is loaded with the periodic ceramic dielectric material which can suppress the spurious oscillations in gyrotron amplifiers. In the present work, the interaction circuit of a ka-band gyro-TWT has been modeled as shown in figure 1 to study the beam-wave interaction mechanism. The interaction region consists of two parts namely long lossy periodically loaded and the conducting unloaded sections. The dielectric material for the loaded section of the model has been chosen as Beryllium Oxide-silicon Carbide (BeO-SiC) with a relative permeability of $\varepsilon_r = 7.11 - j1.1$ and a relative permeability $\mu_r = 1$ and which is a lossy material due to its good thermal conductivity and which is also importance for high average power operation. Another material in the loaded section of the model is set as copper with the conductivity (σ) of 5.8×10^7 S/m without considering surface roughness. The loaded section consists of 18 ceramic rings alternating with copper rings of 3.5 mm length, while the ceramic ring has 8 mm length and the radial thickness of the dielectric ring is 1.5 mm. The unloaded section has 53 mm length. Total length of the interaction circuit is 260 mm [10]. The copper rings are incorporated into the design for ease of assembly and to help collect stray electrons that could potentially cause breakdown

and also, including metal rings allow the loading of non axis symmetric parasitic modes to be adjusted selectively due to the absence of axial currents in the Transverse Electric (TE_{0n}) modes [9].

The tangential component of the Electric field has been set as zero (E_t = 0) all along the boundary of the interaction structure as shown in figure 2. The region of interest has been discretized using hexahedral meshing technique and which is very robust even for most complex imported geometries and also which increases the speed of computations with good accuracy. In figure 3, red dot represents mesh node at a particular position and mesh lines pass through these nodes. Lines per wavelength control the size of mesh shells.

Figure 1: Cross sectional view of the simulation model of gyro-TWT's interaction circuit

2.2 Particle Emission Model

For the beam-wave interaction mechanism, the gyrating electron beam has to be introduced into the periodically loaded cylindrical wave guide interaction region to drive the electromagnetic wave which is also being introduced into the same region. Generally, there are no tools for developing the gyrating electron beam; therefore a special arrangement has to be made in order to produce the gyrating electron beam as shown in figure 4 Particles are emitted from a tilted surface whose angle of tilt is determined from the ratio of transverse velocity of the beam to the axial velocity. Here, the DC beam emission model is taken which requires assigning any of the constant value parameter to the particles as Lorentz factor (γ), normalized velocity (β), velocity (v) or energy (u). These parameters can be calculated as

$$\gamma = 1 + \frac{eV_b}{m_e c^2} \tag{2}$$

$$\beta = \sqrt{1 - \frac{1}{\gamma^2}} \tag{3}$$

$$v = \beta c \tag{4}$$

$$u = (\gamma - 1)\left(\frac{m_e c^2}{e}\right) \tag{5}$$

where, e is charge of the electrons, me is the rest mass of the electrons, c is the velocity of light, V_b is the beam voltage.

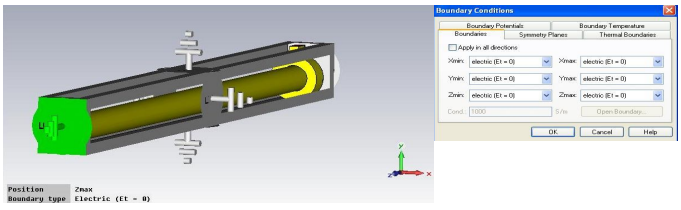

Figure 2: Implementation of boundary conditions around the interaction structure

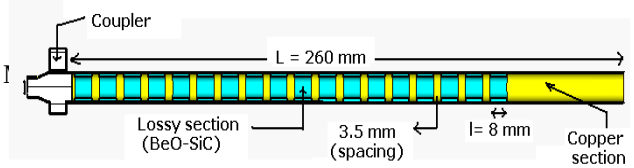

A kinetic spread for the particle emission and its velocity can be introduced based on the quality of the beam obtained separately by analysis/simulation of a magnetron injection gun (MIG). The cathode has the radius of as same as that of the beam radius. Initially, all the particles have been assigned a constant energy value and the current rise time has been taken as 1 ns. A kinetic spread for the beam and current has been defined based on the quality of the beam obtained separately by analysis/simulation of a magnetron injection gun (MIG). For the accuracy of results, 10 numbers of beam lets have been considered. The operation of the waveguide in the desired operating mode and frequency has been monitored by observing the fields. The particles are monitored at regular interval of time over the entire simulation period by observing their energy, momentum, position, etc. This stores the full particle data at the set location, which can be exported for subsequent simulation of collector. For the analysis of electron bunch the energy transfer phenomena, phase space for momentum and position of electrons have been recorded.

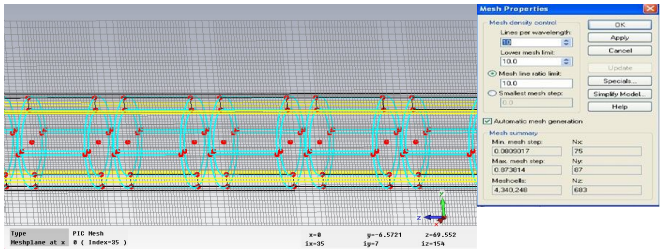

Figure 3: Mesh view of simulation structure with mesh properties.

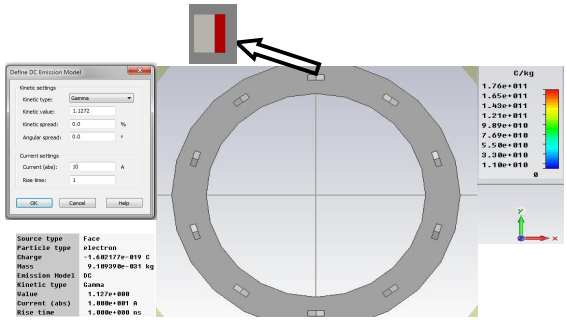

Figure 4: Design of cathode with emitters (indicated by arrow) produces the gyrating electron beam lets

3. RESULTS AND DISCUSSION

3.1 Beam Absent simulation and Loss Rate Calculation

In order to ensure that the device operation is at the desired mode and frequency, beam absent (cold analysis) simulation is performed. Further, for the beam present simulation, the electrons are being considered as uniformly distributed in azimuthal direction in the form of gyrating beamlets and their evolution along the interaction length in the presence of electromagnetic signal is observed in time domain. The space

charge effect of the electron beam has been neglected in the PIC simulation for ease of work. Electrons start to bunch as they drift along the interaction region. Once the electrons are bunched, they transfer their energy to electric field which reverses its direction in each half cycle of the cyclotron frequency in synchronism with the Larmor gyration of the electrons. This makes possible amplification of an electromagnetic wave at the cyclotron frequency. The Fourier transform of time varying field confirmed the desired frequency of operation in hot beam analysis.

The total length of the interaction circuit has been extended by introducing a loaded section, which allows a high gain and stable operation of the Gyro-TWT amplifier. The measured loss rate of the loaded part for the TE_{01} mode is approximately 4.5 dB /cm at 35 GHz and which has very little effect on the output power and bandwidth of the gyro-TWT, while the corresponding loss rate for the gyro-BWO modes TE_{21} is about −12 dB /cm at 28.4 GHz in the loaded section [10]. The periodically loaded circuit consisted of two ceramic rings and a copper ring has been cold analyzed (without beam) in CST Microwave studio. This cold loss rate can also be calculated by using the known loss tangent (tan δ = 0.154) of BeO-SiC. Figure 5 (a) predicts the transmission characteristic of the interaction circuit includes the periodic dielectric loaded section having the length of 2.3 cm through 3-D electromagnetic simulation software. The simulated loss rate of the loaded part for TE_{01} mode operation is ∼4 dB /cm at 35 GHz and which shows that it has got very little effect on the output power and bandwidth of the gyro-TWT, while the corresponding loss rate for the gyro-BWO modes become more than the 10dB /cm. The simulations indicating that this loss rate was sufficient to suppress all oscillations for beam currents of 8–12 A, beam voltages of 65–75 kV, and beam alphas of 1.0–1.5. The figure 5 (b) shows the absolute E-field in the cross section of the interaction region which confirms the propagation of the desired mode inside it.

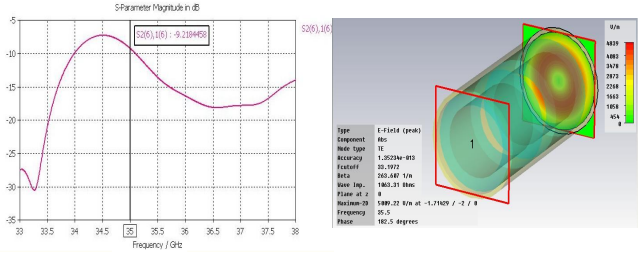

(a) (b)

Figure 5: (a) Transmission characteristic of the loaded section consisting of two ceramic rings and a copper ring (b) Contour plot of TE_{01} Elecrtric field pattern at the output of the loaded section

This loss rate calculation is having significant role in determining the linear stability of the gyro-TWT [15] [16]. The fundamental axial mode of an oscillation is the most threatening spurious oscillation in a uniform circuit [15]–[18]. The linear stability study usually traces the critical length of such a fundamental axial mode according to the variation of the loss strength. The figures 6 (a) and 6 (b) show the tranverse cross section of electric field pattern inside the dielectric (BeO-SiC) and the copper metal ring respectively. The figure 6 (c) shows the longitudinal electric field distribution of the desired mode along the axial direction. The red color represents the positive direction of the longitudinal electric field. The accelerating and retarding electronic fields distribute periodically along the longitudinal direction. This is just a requisite for the beam–wave interaction of microwave wave amplification mechanism. The dielectric loss effectively absorbs the resonant modes and reduces the field strength in the dielectric slots. Due to this absorption, the unwanted higher order harmonic components arising from the structural periodicity are suppressed. Modes propagating in such a lossy periodic system exhibit complex dispersion relations and field distributions. Therefore, the proper and meticulous selection of the waveguide dimension will provide the lowest attenuation for the desired operating TE_{01} mode while maintaining a strong enough attenuation of the competing potentially unwanted modes in order to ensure stable gyro-TWT operation.

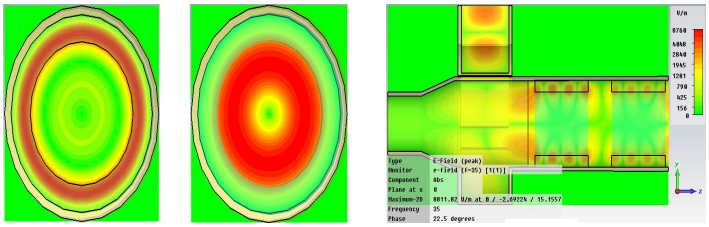

(a) (b) (c)

Figure 6: Contour of Electric field pattern (a) inside the ceramic (BeO-SiC) ring of 1.5 mm thickness (b) inside the waveguide (metal ring) and (c) Contour of the Electric field pattern of TE_{01}- mode along the axial direction of interaction circuit

3.2 Beam Wave Interaction Characteristics

The circuit includes input coupler, interaction region (both loaded and unloaded section) and output port and which has been a physical model of the dielectric loaded gyro-TWT in order to make it stable. The spiraling electron beam is produced by the current density source. The EM field action changes the electron relativistic factor (γ), depending on the electron phase relative to the wave, and results in phase slippage and bunching, with the corresponding current driving the wave in turn. As the EM wave and the gyrating electron beam move down the interaction space, the kinetic energy of the electron beam is transferred to the electromagnetic fields, hence the amplification. The amplified EM is emanated out through the output port where the electron is terminated. Particles have been directly

absorbed on the surface of metal neglecting secondary electron emission. The magnetic field is one of the crucial factors in the beam wave interaction. It determines the coupling strength of the beam wave interaction. An increase in magnetic field may enhance the output power at higher frequency but reduce the output power at the lower frequency due to the excessive saturation of the beam wave interaction. Furthermore, an increase in magnetic field will easily lead to instability of the gyro-TWT. Additionally, in the present case a uniform longitudinal magnetic field of 1.24 T has been used here to lead the spiraling electron beam. Here 10 beamlets have been considered for our simulation due to memory constraints. The Table 3.1 gives the specifications of the Gyro-TWT for the hot beam analysis [10]. The simulation time has been set as 100 ns which is good enough for amplifier stabilty and five modes have been taken into account to show the mode competition phenomena in a ka band Gyro-TWT. Subsequently, the 3-D CST Particle in Cell (PIC) electromagnetic code has been used to substantiate the beam wave interaction simulation mechanism.

In order to improve the accuracy in PIC simulation one should choose the mess size wisely. The lines per wavelength and the mess size should be kept as small as possible so as to have better accuracy along with lesser simulation time. We have used automatic mess generation technique in which lines per wavelength has been set as 10. The automated mess generation provides minimum mess step size 0.08 mm and maximum step size 0.87 mm which correspond to 43,40,248 number of mess cells. The total no of electrons coming out from cathode in the whole simulation time is 55, 34,110. The electron trajectory of beamlets has been shown in figure 7 (a) and in this process electron bunches are formed by interacting with the transverse electric field and also which shows the phase variation of the electrons form the input port to the output port during the interaction process.

Table 1: Design Parameters of Gyro-TWT Amplifier

Electron Beam Voltage	70 keV
Electron Beam current	10 A
Operating mode	TE_{01}
Operating frequency	35 GHz
Cut off frequency	33.26 GHz
Velocity pitch, α	1
Axial velocity spread	5 %
Magnetic field, B_0	1.24 Tesla
Circuit radius, R_w	5.5 mm
Guiding center radius, R_g	0.48 R_w
Lossy circuit length	207 mm
Copper circuit length	53 mm
Total length	260 mm

(a)

Figure 7: (a) shows the trajectory of electron from input port to output port during interaction (side view), Front view of electron beam with 10 beamlets (b) before Interaction, (c) after interaction (inset shows a zoomed beamlet)

The figure 7 (b) shows that at the entrance of the interaction circuit the electronic transverse momentum has been uniformly distributed which means that macro particles have the same energy and uniform phase distribution and also shows that the Larmor radius of all beamlets is same. After beam-wave interaction, a center of bunch has been formed and the electrons are not uniformly distributed on the gyrating orbit and this is depicted in figure 7 (c). This is enhanced in the loaded section of the interaction region and in the nonlinear amplification region the driver wave is getting amplified while the electrons lose their kinetic energy. The driver signal to the input coupler is 100 W which is shown in figure 8 (a) and the figure 8 (b) shows the actual power coupled to the beam which has the strength of 10 W.

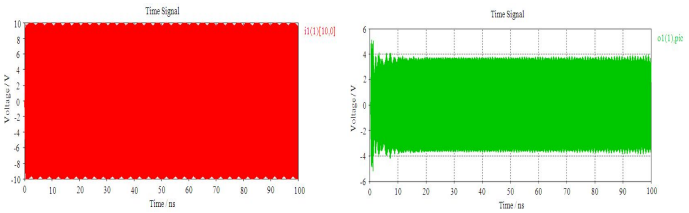

(a) (b)

Figure 8: (a) Driver input signal applied to the coupler (100 Watts) and (b) Coupled signal to the beam (10 Watts developed)

The evolution of the EM signal at the output port of the interaction circuit with respect to time has been shown in figure 9 (a) and 9 (b) for the desired mode and other nearby competing modes. It has also been observed that the growth of EM power approaching the saturation level at a time beyond 30 ns. After the template based post processing in CST particle studio the output power has been calculated as 175 kW approximately at 35 GHz and which has been shown in figure 10 (a). The electronic efficiency has been calculated as 25 % for 70 keV, 10 A annular electron beams with a velocity pitch of 1.0 and the gain of the device has been about 42.43 dB. The 3 dB instantaneous band-width has also been

computed as 6.17%.

In figure 10 (b), the frequency spectrum of azimuthal electric field has been shown which is obtained by taking the Fourier transform of the electric field. Obviously, it is characterized by a single-frequency component, peaked at 35 GHz. This validates the frequency of operation of the gyro- TWT. Moreover, the figure 9 (a) and (b) show the comparison of power distribution in nearby spurious competing modes like TE_{11}, TE_{21}, TE_{31} and TE_{41} against the desired TE_{01} mode. This plot evident that no mode is getting sufficient power to compete the desired operating mode and it is also shown that no mode is grown more than 250 Watts compared to our desired operating mode which is grown to 175 kW. It is important to note that the backward mode TE_{21} is dangerous for the stability of Gyro-TWT and which has been grown below 220 Watts only. This is an advantage of the distributed lossy interaction structure.

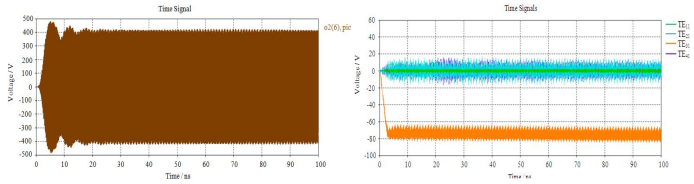

(a) (b)

Figure 9: (a) Temporal response of signal developed for TE_{01} at the output of the interaction circuit and (b) Temporal response of signal for various spurious competing modes

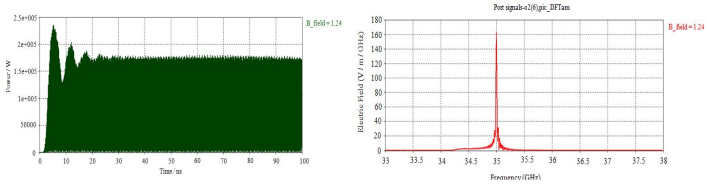

(a) (b)

Figure 10: (a)Temporal output power growth at the end of interaction structure for TE_{01} mode and (b) frequency spectrum of probe signal. DFT spectrum of the electric field depicts the operating point of a 35 GHz Gyro-TWT

4. PARAMETRIC ANALYSIS AND VALIDATION

With the help of the CST particle simulation code, the variation of the output power has been observed with respect to the beam pitch factor (α), beam velocity spread ($\Delta v_z/v_z$), the input powers and frequencies for the fixed static magnetic field (B_0) values. Obviously, with increasing velocity spread, the output power decreases and this happens because some particles have lower kinetic velocities and hence transfer lesser amount of energy to the EM wave which has been shown in figure 12. The maximum power growth has been observed in TE_{01} mode and other modes are contained much less amount of power, which is shown in figure 9.

The applied DC magnetic field is being kept constant throughout the length of the interaction region and also the simulation time. The CST particle simulation code accounting the multiple mode oscillations present in the waveguide interaction structure and the EM power growth in all the other nearby competing spurious unwanted modes that can be observed as shown in figure 9. As the presence of competing modes is inevitable in a conventional waveguide, consideration of the nearby competing modes provides more realistic picture of the beam-wave interaction mechanism. Obviously, for the present study of gyro-TWT, the output power has been obtained as 175 kW. This is in close agreement with the published results [10] as shown in figure 14. The 3 dB instantaneous bandwidth of the amplifier has been calculated as 2.16 GHz. Further, the output power of the ka-band Gyro-TWT has been computed for various input powers. This is shown in figure 15 and which is evident that the saturated gain of the amplifier as 42.43 dB for 10 Watts

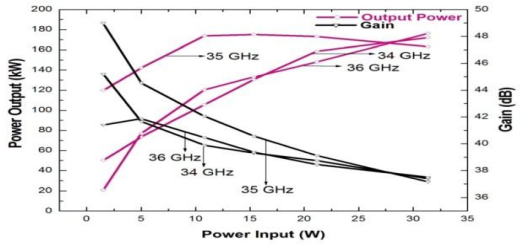

input power. The electronic efficiency of the amplifier has been calculated as 25% for 70 keV, 10 A electron beam.

Figure 11: Variation of output power and gain with respect to input power for various input frequencies

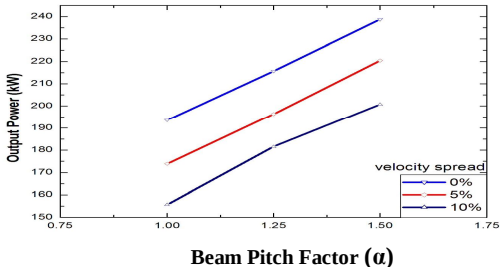

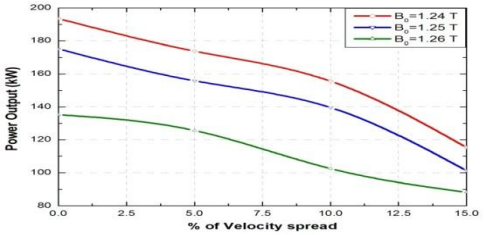

Figure 12: Variation of output powewr with respect to pitch ratio for different spreads

Figure 13: Variation of Output power with respect to velocity spreads for the applied magnetic fields

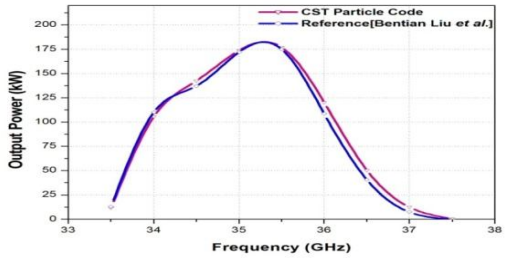

Figure 14: Variation of Power Output with respect to input frequencies of Ka- band Gyro-TWT.

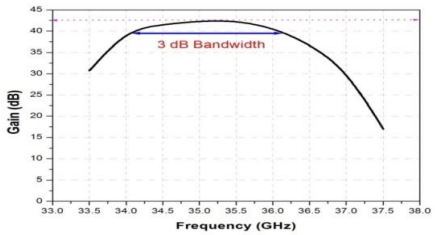

Figure 15: Calculated gain for a Ka-band gyro-TWT Amplifier

5. CONCLUSION

Beam-wave interaction mechanism in a Ka-band periodcally ceramic loaded gyro-TWT amplifier has been investigated using PIC simulation. A novel technique of generating gyrating electron beam has been demonstrated and the beamlets observed at the end of simulation shows the bunching phenomena of the particles. The energy contained in all the particles along the interaction region responsible for the net output power growth is obtained by the energy transfer from the electron beam to the RF wave. The simulation takes some finite time to settle in the TE_{01} mode of operation due to the competition from nearby spurious modes. The simulations predict that the peak output power in dielectric loaded gyro-TWT as 175 kW at 35 GHz corresponding to power conversion efficiency of 25%, when a 70 keV, 10 A annular electron beams with a perpendicular to parallel electron velocity ratio of 1.0. The gain of the device has been obtained ~ 42 dB for the input power of 10 Watts. The 3 dB instantaneous bandwidth is found ~ 6%. PIC simulation also show that no appreciable power in the other modes except the desired TE_{01} mode throughout the operation which confirms the mode suppression. The DFT spectrum of the recorded electric field has a single peak at 35 GHz which substantiates the intended device desired operating frequency. The higher value of velocity spread of the electron beam reduces the power output. The stability of this device was excellent, demonstrating that the ceramic loading is a highly effective means of suppressing spurious oscillations in gyro-TWTs.

It is hope that present study would be useful in validating the earlier experimental findings and understanding the electron beam and RF wave interaction mechanism in the gyro-TWT.

REFERENCES

1. K. R. Chu. **The electron cyclotron maser**, Review of Modern Physics, vol. 76, no. 2, pp. 489-540, April 2004.
2. Zhiliang Li, Jinjun Feng, Efeng Wang and Bentian Liu. **Study of a Wband Second-Harmonic Gyro-TWT Amplifier**, IEEE conference, international, pp 335-336, 2011.
3. L. R. Barnett, K. R. Chu, J. M. Baird, V. L. Granatstein, and A. T. Drobot. **Gain, saturation, and bandwidth measurements of the NRL gyrotron traveling-wave amplifier**, in *IEEE IEDM Tech. Dig.*, 1979, pp. 164–167.
4. Y. Y. Lau, K. R. Chu, L. R. Barnett, and V. L. Granatstein. **Gyrotron travelling wave amplifier: I. Analysis of oscillations**, *Int. J. Infrared Millimeter Waves*, vol. 2, pp. 373–393, 1981.
5. L. R. Barnett, J. M. Baird, Y. Y. Lau, K. R. Chu, and V. L. Granatstein. **A high gain single stage gyrotron traveling-wave amplifier**, in *IEEE IEDM Tech. Dig.*, 1980, pp. 314–317.
6. Q. S. Wang, D. B. McDermott, N. C. Luhmann, Jr.. **Operation of a stable 200 kW second harmonic gyro-TWT amplifier**, IEEE Trans.Plasma Sci. 24(3), 700 (1996).
7. K. R. Chu, H. Y. Chen, C. L. Hung, T. H. Chang, L. R. Barnett, S. H. Chen, T. T. Yang, and D. J. Dialetis. **Theory and experiment of ultrahigh- gain gyrotron traveling wave amplifier**, *IEEE Trans. Plasma Sci.*, vol. 27, pp. 391–404, Apr. 1999.
8. V. L. Bratman, A. W. Gross, G. G. Denisov, W. He, A.D. Phelps , K. Ronald , S.V. Samsonov , C.G. Whyte , A.R. Young . **High-Gain Wide-Band Gyrotron Traveling Wave Amplifier with a Helically Corrugated Waveguide**, Phys. Rev. Lett. 84, 2746 (2000).
9. J. P. Calame, M. Garven, B. G. Danly, B. Levush, and K. T. Nguyen. **Gyrotron-traveling wave-tube circuits based on lossy ceramics**, *IEEE Trans. Electron Devices*, vol. 49, no. 8, pp. 1469–1477, 2002.
10. Bentian Liu, Jinjun Feng, Efeng Wang, Zhiliang Li, Xu Zeng, Lijun Qian, and Hui Wang. **Design and Experimental Study of a Ka-band Gyro-TWT With Periodic Dielectric Loaded Circuits**, *IEEE Transactions on Plasma Science*, vol. 39, no. 8, 2011.
11. J. Schneider. **Stimulated emission of radiation by relativistic electrons in a magnetic field**, Phys. Rev. Lett., vol. 2, pp. 504–505, 1959.
12. A. K. Ganguly and S. Ahn. **Large-signal theory of a two-stage wideband gyro-TWT**, IEEE Trans. Electron. Devices, pp. 474–480, Apr.1984.
13. K. T. Nguyen, J. P. Calame, D. E. Pershing, B. G. Danly, M. Garven,B. Levush, and T.M. Antonsen Jr. **Design of**

a Ka-band gyro-TWT for radar applications, IEEE Trans. Electron Devices, vol. 48, pp. 108–115,Jan. 2001.

14. T.M. Antonsen Jr., A. A.Mondelli, B. Levush, J. P. Verboncoeur, and C.K. Birdsall. **Advances in modeling and simulation of vacuum electronic devices**, Proc. IEEE, vol. 87, pp. 804–839, May 1999.
15. C. L. Hung. **Linear Analysis of a Coaxial-Waveguide Gyrotron Traveling Wave Tube**, *Phys. Plasmas*, vol. 13, no. 3, p. 033 109, Mar. 2006.
16. C.H. Du, P. K. Liu, Q. Z. Xue, and M. H. Wang. **Effect of a Backward-Wave on the Stability of an Ultrahigh Gain Gyrotron Traveling Wave Amplifier**, *Phys. Plasmas*, vol. 15, no. 12, p. 123 107, Dec. 2008.
17. T. H. Chang and N. C. Chen. **Transition of Absolute Instability from Global to Local Modes in a Gyrotron Traveling Wave Amplifier**, Phys. Rev. E, Stat. *Phys. Plasmas Fluids Relat. Interdiscip. Top.*, vol. 74, no. 1,p. 016 402, Jul. 2006.
18. C. H. Du and P. K. Liu. **Stability Study of a Gyrotron Traveling Wave Amplifier Based on a Lossy Dielectric Loaded Mode Selective Circuit**, *Phys. Plasmas*, vol. 16, no. 7, p. 073 104, Jul. 2009.